Journal of Materials Chemistry A

PAPER

View Article Online
View Journal | View Issue

Cite this: J. Mater. Chem. A, 2014, 2, 1790

Bond strength dependent superionic phase transformation in the solid solution series $Cu_2ZnGeSe_{4-x}S_x$

Wolfgang G. Zeier,†[ab] Christophe P. Heinrich,†[a] Tristan Day,[b] Chatr Panithipongwut,[b] Gregor Kieslich,[a] Gunther Brunklaus,[c] G. Jeffrey Snyder*[b] and Wolfgang Tremel*[a]

Received 1st August 2013
Accepted 23rd November 2013

DOI: 10.1039/c3ta13007j

www.rsc.org/MaterialsA

Recently, copper selenides have shown to be promising thermoelectric materials due to their possible superionic character resulting from mobile copper cations. Inspired by this recent development in the class of quaternary copper selenides we have focused on the structure-to-property relationships in the solid solution series $Cu_2ZnGeSe_{4-x}S_x$. The material exhibits an insulator-to-metal transition at higher temperatures, with a transition temperature dependent on the sulfur content. However, the lattice parameters show linear thermal expansion at elevated temperatures only and therefore no indication of a structural phase transformation. ^{63}Cu nuclear magnetic resonance shows clear indications of Cu located on at least two distinct sites, which eventually merge into one (apparent) site above the phase transformation. In this manuscript the temperature dependent lattice parameters and electronic properties of the solid solution $Cu_2ZnGeSe_{4-x}S_x$ are reported in combination with ^{63}Cu NMR, and an attempt will be made to relate the nature of the electronic phase transformation to a superionic phase transformation and a changing covalent character of the lattice upon anion substitution in this class of materials.

1 Introduction

Copper selenide based materials have recently attracted interest in the field of thermoelectric materials due to their very low thermal conductivities. While the mobile copper cations result in a "phonon-liquid electron crystal" type behavior in this class of superionic materials resulting in low heat capacities,[1,2] the inherent structural disorder leads to low thermal conductivities in compounds such as $Cu_2Zn(Sn/Ge)Se_4$ (ref. 3–8) and CuGaSe(Te)$_2$.[9,10] These properties are a direct result from the structure and bonding environment and a thorough understanding of the structural properties is necessary in order to design new thermoelectric materials.[11]

Especially the quaternary copper chalcogenides provide great opportunities to study the influence of structure and bonding on the transport properties. For example, $Cu_2ZnSnSe_{4-x}S_x$ and related compounds have attracted attention for their use in photovoltaics, due to possible band gap tuning, with metal–sulfur interactions leading to larger band gaps.[12–15] Furthermore it has been shown that different bonding environments, bond angles and bond lengths can lead to an increased scattering of phonons.[8]

The structure of the stannite-type solid solution series $Cu_2ZnGeSe_{4-x}S_x$ (space group $I\bar{4}2m$) is shown in Fig. 1. Structurally derived from the diamond structure, these multinary chalcogenides form when the substructures are populated with different cations. This ordered substitution doubles the translational period along the z-direction resulting in tetragonal symmetry; different metal–anion interactions induce a tetragonal distortion with a $c/(2a)$-ratio < 1.[16] Zn occupies the Wyckoff position 2a (0,0,0), and Ge is located on site 2b (0,0,1/2), and therefore sharing a plane in this structure. Cu resides on the Wyckoff position 4d (0,1/2,1/4) forming slabs of Cu–Se tetrahedra.[17]

Inspired by a recently observed insulator-to-metal transition in the $Cu_2ZnGeSe_4$ compound,[7] and the possibility of tuning the covalent character due to substitution of selenium with sulfur,[12–15] we explored the effect of the lattice and bonding on the transport properties of this phase transformation. We show that within the solid solution series $Cu_2ZnGeSe_{4-x}S_x$ an insulator-to-metal transition occurs; an increase of the transition temperature occurs upon substituting selenium by sulfur. Whereas high temperature X-ray diffraction data are inconclusive concerning a structural phase transformation, ^{63}Cu nuclear magnetic resonance (NMR) provides clear indications of Cu located on two distinct sites, merging into one site above the

[a]Institut für Anorganische Chemie und Analytische Chemie der Johannes Gutenberg-Universität, Duesbergweg 10-14, D-55099 Mainz, Germany
[b]Materials Science, California Institute of Technology, 1200 E. California Blvd, Pasadena, CA 91125, USA
[c]Institut für Physikalische Chemie, Westfälische Wilhelms-Universität Münster, Corrensstraße 28/30, D-48149 Münster, Germany
† These authors contributed equally to this manuscript.

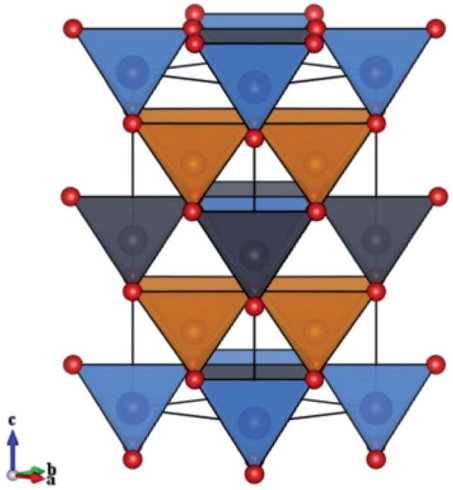

Fig. 1 Crystal structure of the stannite type $Cu_2ZnGeSe_{4-x}S_x$. Cu atoms are indicated by orange, Ge atoms are indicated by gray, Zn atoms are indicated by blue, and Se/S atoms are indicated by red, with the tetrahedral coordination of the elements indicated. Note the difference in the ordering of the metal cations. While Zn and Ge share a plane in this structure, Cu resides on the 4*d*-Wyckoff position (0,1/2,1/4) alone, forming slabs of Cu–Se-tetrahedra.

phase transformation temperature. An attempt will be made to relate the electronic properties to a superionic phase transformation, which depends on a gradually changing covalent bonding character upon anion substitution.

2 Experimental

Bulk samples of polycrystalline $Cu_2ZnGeSe_{4-x}S_x$ with compositions $x = 0, \ldots, 4$ were prepared *via* solid state reactions using elemental powders of Cu (Alfa Aesar, 99.999%), Zn (Sigma Aldrich, 99.995%), Ge (Chempur, 99.99%), Se (Alfa Aesar, 99.999%) and pieces of S (Alfa Aesar, 99.999%). A sublimation–deposition procedure of the ground sulfur was used to ensure dry conditions. The phase purity of the starting materials was verified by X-ray diffraction, and all synthetic procedures were carried out in a N_2 dry box. Annealing was performed in evacuated quartz ampoules, which were preheated at 1073 K under dynamic vacuum for 5 hours to ensure dry conditions.

The starting elements were thoroughly ground, sealed in quartz ampoules, and annealed in a first step at 923 K for 48 hours ($x = 0$) and 96 hours for $x \geq 1$. In the following second step, the harvested powders were ground again, re-sealed and re-annealed for 96 hours at 1073 K and 973 K. Heating and cooling rates for all procedures in the horizontal tube furnaces were 5 K min^{-1}. The different synthetic temperatures are due to a structural phase transformation at 1063 K, which occurs in the sulfur containing members of this series.[18] It was found that the second annealing step was necessary to prevent the formation of the binary and ternary compositions. The quartz ampoules were 10–12 cm in length and 11 mm in inner diameter with a maximum amount of 1.5 g of starting materials within the ampoule. This ampoule geometry was found to prevent a significant loss of selenium at higher temperatures, indicated by red selenium precipitation present in longer ampoules. The obtained powders of $Cu_2ZnGeSe_{4-x}S_x$ were hand ground and consolidated into 1–1.5 mm thick, 12 mm diameter disks at 873 K for 5 hours ($x = 0$), 1073 K for 6 hours ($x = 1$), and 973 K for 6 hours ($x \geq 2$) under a pressure of 40 MPa by induction hot pressing in high density graphite dies.[19] The resulting samples have more than 95% theoretical density, determined from the mass and geometry of the consolidated disks.

Room temperature X-ray diffraction measurements were performed on a Siemens D5000 powder diffractometer with a Braun M50 position sensitive detector and $CuK_{\alpha 1}$ radiation (Ge (220) monochromator) with a step size of 0.0078° in 2Θ. Variable temperature X-ray diffraction for $Cu_2ZnGeSe_4$ was performed on a Philips PANalytical X'Pert Pro with CuK_α radiation and a step size of 0.0084° in 2Θ and a Seifert XRD 3000 P with CuK_α radiation and a step size of 0.02° in 2Θ was used for the sulfur containing compounds. Pawley refinements were performed with TOPAS Academic V4.1,[20] applying the fundamental parameter approach using the crystallographic data from Schäfer and Nitsche.[17] The instrumental measurement uncertainty for the determination of the lattice parameters at room temperature is approximated to be 0.003 Å.

The ^{63}Cu MAS NMR spectra were recorded with a Bruker Advance 500 spectrometer using a special high-temperature Bruker WVT 4 mm double-resonance probe, operating at 132.64 MHz, and a rotor frequency of 10 kHz while applying temperatures ranging from 300 K to 523 K (bearing gas nitrogen, ±5 K). For each spectrum 16 384 transients were averaged with a relaxation delay of 0.2 s and a pulse length of 1.5 μs (B_1-field: 83.3 kHz).

The Seebeck coefficient was calculated from the slope of the voltage *vs.* temperature gradient measurements from Chromel–Nb thermocouples, applying a temperature gradient of 10 K.[21] Electrical resistivity was measured using the van der Pauw technique under a current of 20 mA, and pressure-assisted contacts. All measurements were performed under dynamic vacuum and on multiple samples for each composition. The measurement data shown include the data collected during heating and cooling.

3 Results and discussion

All samples were checked for phase purity prior to any transport measurements; the respective X-ray diffraction data have been shown elsewhere.[7] Rietveld refinements of the room temperature diffraction data show site occupancies of Cu^+ and Zn^{2+} significantly below 100%, with the missing electron density found on the interstitial sites. However, due to the very similar scattering form factors for X-rays Cu^+ and Zn^{2+} cannot be distinguished *via* X-ray diffraction. Powder X-ray diffraction data of samples prior to the hot pressing procedure and data taken from consolidated samples do not show any significant texture in this material. Therefore, properties measured on disks of this polycrystalline material are expected to be isotropic within expected experimental uncertainty and represent a scalar average of the tensor properties. Fig. 2 shows refined lattice

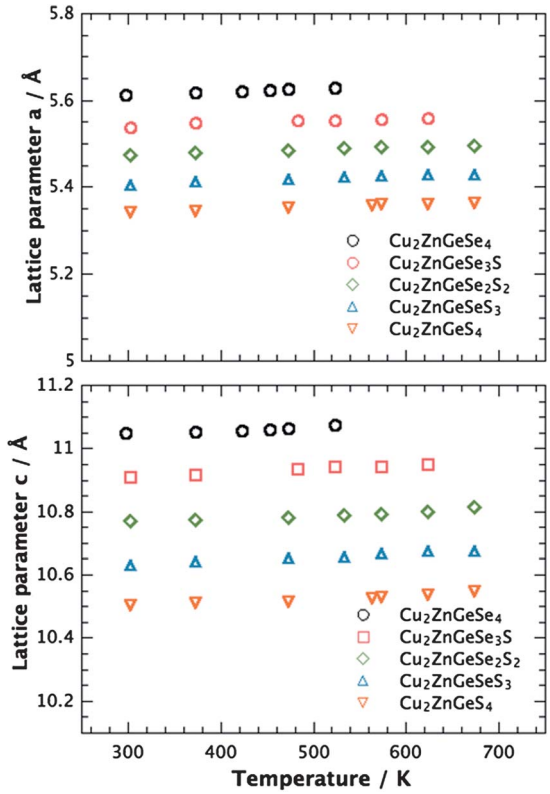

Fig. 2 Lattice parameter *a* (top) and *c* (bottom) of $Cu_2ZnGeSe_{4-x}S_x$ as a function of temperature. The lattice parameters increase linearly with temperature as a result of the thermal expansion of the lattice. A structural phase transformation would be visible as a change of slope (or kink) in the data. The lattice parameters follow Vegard's law, showing a decrease of *a* and *c* with increasing sulfur content due to the smaller S atom in the lattice.

parameters of the solid solution series $Cu_2ZnGeSe_{4-x}S_x$, using Pawley refinements, as a function of temperature. Substitution of Se by S results in a decrease of the lattice parameters *a* and *c*, following Vegard's law as a result of the smaller ionic radius of sulfur compared to selenium. The lattice parameters increase linearly with temperature due to thermal expansion of the lattice and no structural phase transformation can be observed which would be visible as a change of slope in the data. However, a small exothermic effect can be detected *via* differential scanning calorimetry.[7]

^{63}Cu magic angle spinning (MAS) NMR spectra of $Cu_2ZnGeSe_4$ indicate the presence of at least two distinct Cu cation sites below 450 K whose second-order quadrupolar line shapes cannot be deconvoluted unambiguously owing to the conflicting demands of increased resolution (faster spinning) and high temperatures. Above 450 K, a broad featureless line shape was observed. In the stannite crystal structure type of $Cu_2ZnGeSe_4$, however, Cu is merely located on a single crystallographic site, Wyckoff position 4*d* (0,1/2,1/4). Therefore, a combination of the significantly lower site occupancy of Cu and the ^{63}Cu-NMR data strongly suggests interstitial Cu^+ occupation in this compound. With increasing temperature, all Cu cations become rather mobile leading to a superionic phase transformation at 450 K. Above the superionic transition temperature, the cation mobility results in partially averaged local electric field gradients at the copper site, as reflected by the ^{63}Cu MAS NMR line shape (Fig. 3).

Temperature dependent resistivities (see Fig. 4) reveal an insulator-to-metal transition, which has been initially observed for the selenium compound.[7] While the resistivity decreases with increasing temperature below the phase transformation it starts to increase afterwards. Temperature dependent positive Seebeck coefficients (Fig. 5) show p-type intrinsic semiconducting behavior below the phase transformation, and the transition is visible as a minimum in the thermopower. Differences in the values of the thermopower of the different

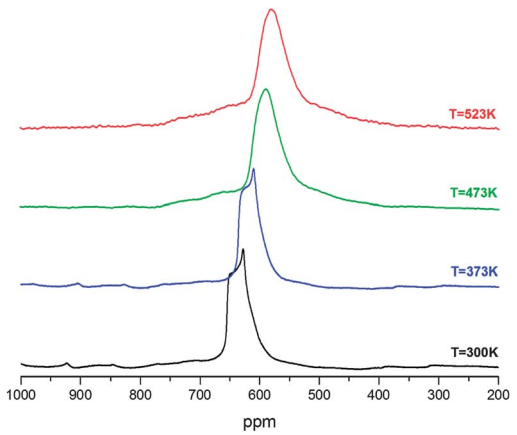

Fig. 3 ^{63}Cu magic angle spinning nuclear magnetic resonance of the stannite type $Cu_2ZnGeSe_4$ at different temperatures below and above the phase transformation at 450 K. The signal at lower temperatures shows at least two distinct lattice sites (whose second order quadrupolar line shapes cannot be unambiguously extracted) that later merge into one (apparent) site for Cu, thus suggesting mobile Cu cations due to a superionic phase transformation.

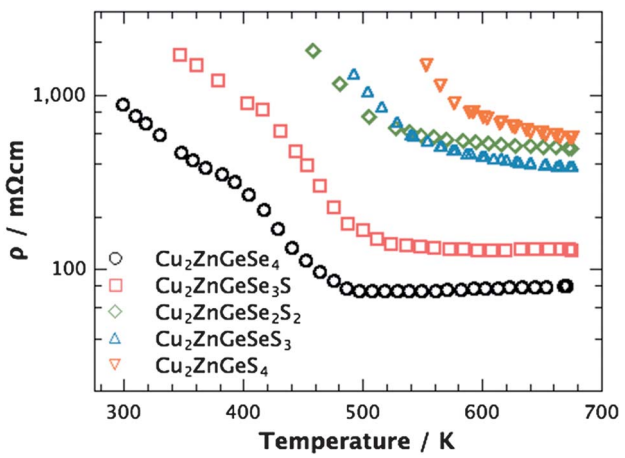

Fig. 4 Resistivity ρ of $Cu_2ZnGeSe_{4-x}S_x$ as a function of temperature. At lower temperatures the solid solution series exhibit insulating properties, while the change of slope at higher temperatures reveals the existence of an insulator-to-metal transition. The transition temperature and the magnitude of the resistivity increase with increasing sulfur content due to the changing covalent character of the lattice.

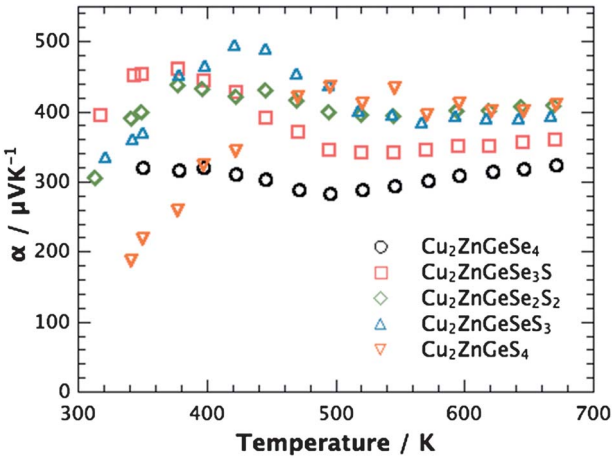

Fig. 5 Seebeck coefficients α of $Cu_2ZnGeSe_{4-x}S_x$ as a function of temperature. While the values of the Seebeck coefficients are mainly governed by intrinsic defects, the change of slope in combination with a minimum at higher temperatures reveals an electronic phase transformation in this material. The transition temperatures increase with increasing sulfur content.

compositions are due to a combination of the changing band gaps and intrinsic carriers from defects.[8] A control of the charge carrier concentration resulting from intrinsic defects has been shown to be difficult in this class of materials.[8]

The increasing sulfur content leads to an increase of the resistivities of the compounds, which can easily be understood by the changing covalent bonding character in this material and the effect of the differences in charge carrier concentrations from defects.[8,22] A smaller selenium content results in a lower degree of covalent bonding because of the difference in electronegativity compared to sulfur. This leads to very low carrier mobilities due to localization in this structural environment and therefore higher electrical resistivities.[7]

The electrical resistivities and Seebeck coefficients show an increase in the transition temperature of the unknown insulator-to-metal phase transformation, while the temperature dependent lattice parameters show the thermal expansion of the lattice only. In addition, the phase transformation becomes less pronounced. The nature of this phase transformation may be understood considering the possible interstitial occupancy of copper and the missing electron density on the specific lattice sites. Below the temperature of the phase transformation only holes from intrinsic defects contribute to the transport. At a certain temperature the bonding attraction between the copper ions and the anions can be overcome by the thermal energy and copper ions start to become mobile leading to an increase in the resistivity with temperature and an increase of the Seebeck coefficient. While this mechanism cannot be detected by standard laboratory X-ray diffraction the exothermic effect in the differential scanning calorimetry supports the idea of a superionic phase transformation.[2,7] The increase in the transition temperature with increasing sulfur content results from the lower degree of covalent bonding from the sulfur. With increasing ionicity the copper is more strongly bonded to the lattice, and higher temperatures are needed to overcome this energy barrier. This energy-activated behavior can be seen in many ionic conductors.[2]

4 Conclusions

In conclusion we have investigated the electronic properties of the solid solution $Cu_2ZnGeSe_{4-x}S_x$. The lattice parameters follow Vegard's law and increase linearly with temperature due to thermal expansion of the lattice. A previously reported insulator-to-metal phase transformation has been identified in this solid solution, showing a temperature dependence of the transition temperature. ^{63}Cu MAS NMR reveals clear indications of Cu ions located on at least two distinct sites, proposing a superionic transition as a mechanism for this phase transformation due to mobile copper cations. As the nature of the chemical bonding changes due to a changing degree of covalency due to the sulfur ions, this work shows the superionicity of the $Cu_2ZnGeSe_4$ compounds and the influence of the chemical bonding and the structure on the transport properties of thermoelectric materials.

Acknowledgements

Financial support through the Excellence Initiative (DFG/GSC 266) is acknowledged by W. G. Z., C. P. H. and G. K. W. G. Z. is a recipient of a fellowship from the Carl Zeiss-Stiftung. G.K. is a recipient of a fellowship from the Konrad Adenauer Stiftung. T.D. acknowledges support from the U.S. Air Force Office of Scientific Research.

Notes and references

1 H. Liu, X. Shi, F. Xu, L. Zhang, W. Zhang, L. Chen, Q. Li, T. Day, C. Uher and G. J. Snyder, *Nat. Mater.*, 2012, **11**, 422–425.
2 J. Boyce and B. Huberman, *Phys. Rep.*, 1979, **51**, 189–265.
3 X. Y. Shi, F. Q. Huang, M. L. Liu and L. D. Chen, *Appl. Phys. Lett.*, 2009, **94**, 122103.
4 M.-L. Liu, I.-W. Chen, F.-Q. Huang and L.-D. Chen, *Adv. Mater.*, 2009, **21**, 3808–3812.
5 M.-L. Liu, F.-Q. Huang, L.-D. Chen and I.-W. Chen, *Appl. Phys. Lett.*, 2009, **94**, 202103.
6 C. Sevik, *Appl. Phys. Lett.*, 2009, **95**, 112105.
7 W. G. Zeier, A. Lalonde, Z. M. Gibbs, C. P. Heinrich, M. Panthöfer, G. J. Snyder and W. Tremel, *J. Am. Chem. Soc.*, 2012, **137**, 7147–7154.
8 W. G. Zeier, Y. Pei, G. Pomrehn, T. Day, N. A. Heinz, C. P. Heinrich, G. J. Snyder and W. Tremel, *J. Am. Chem. Soc.*, 2013, **135**, 726–732.
9 T. Plirdpring, K. Kurosaki, A. Kosuga, T. Day, S. Firdosy, V. Ravi, G. J. Snyder, A. Harnwunggmoung, T. Sugahara, Y. Ohishi, H. Muta and S. Yamanaka, *Adv. Mater.*, 2012, **24**, 3622–3626.
10 Y. Li, Q. Meng, Y. Deng, H. Zhou, Y. Gao, Y. Li, J. Yang and J. Cui, *Appl. Phys. Lett.*, 2012, **100**, 231903.
11 G. J. Snyder and E. S. Toberer, *Nat. Mater.*, 2008, **7**, 105–114.
12 T. K. Todorov, K. B. Reuter and D. B. Mitzi, *Adv. Mater.*, 2010, **22**, E156–E159.

13 K. Tanaka, Y. Fukui, N. Moritake and H. Uchiki, *Sol. Energy Mater. Sol. Cells*, 2010, **95**, 838–842.
14 K. Wang, B. Shin, K. B. Reuter, T. Todorov, D. B. Mitzi and S. Guha, *Appl. Phys. Lett.*, 2011, **98**, 051912.
15 H. Wei, Z. Ye, M. Li, Y. Su, Z. Yang and Y. Zhang, *CrystEngComm*, 2011, **13**, 2222.
16 S. Schorr, *Thin Solid Films*, 2007, **515**, 5985–5991.
17 W. Schäfer and R. Nitsche, *Mater. Res. Bull.*, 1974, **9**, 645–654.
18 K. Doverspike, K. Dwight and A. Wold, *Chem. Mater.*, 1990, **2**, 194–197.
19 A. D. LaLonde, T. Ikeda and G. J. Snyder, *Rev. Sci. Instrum.*, 2011, **82**, 025104.
20 A. Coelho, *TOPAS Academic V4.1*, 2004.
21 S. Iwanaga, E. S. Toberer, A. LaLonde and G. J. Snyder, *Rev. Sci. Instrum.*, 2011, **82**, 063905.
22 W. G. Zeier, T. Day, E. Schechtel, G. J. Snyder and W. Tremel, *Funct. Mater. Lett.*, 2013, **6**, 1340010.